ISSN 1674-1056
http://cpb.iphy.ac.cn
http://iopscience.iop.org/cpb
中国物理 B
Chinese Physics
中国物理 Chinese Physics B

Effect of strain on exciton dynamics in monolayer WS_2

Lu Zhang(张璐), Da-Wei He(何大伟), Jia-Qi He(何家琪), Yang Fu(付洋), Yong-Sheng Wang(王永生)

Citation: Chin. Phys. B . 2019, 28(8): 087201. **doi:** 10.1088/1674-1056/28/8/087201
Journal homepage: http://cpb.iphy.ac.cn; http://iopscience.iop.org/cpb

What follows is a list of articles you may be interested in

Biaxial strain-induced enhancement in the thermoelectric performance of monolayer WSe_2

Wanhuizi Shen(沈婉慧子), Daifeng Zou(邹代峰), Guozheng Nie(聂国政), Ying Xu(许英)
Chin. Phys. B . 2017, 26(11): 117202. **doi:** 10.1088/1674-1056/26/11/117202

Ultrafast interlayer photocarrier transfer in graphene-$MoSe_2$ van der Waals heterostructure

Xin-Wu Zhang(张心悟), Da-Wei He(何大伟), Jia-Qi He(何佳琪), Si-Qi Zhao(赵思淇), Sheng-Cai Hao(郝生财), Yong-Sheng Wang(王永生), Li-Xin Yi(衣立新)
Chin. Phys. B . 2017, 26(9): 097202. **doi:** 10.1088/1674-1056/26/9/097202

Enhancing redshift phenomenon in time-resolved photoluminescence spectra of AlGaN epilayer

Wei Li(李维), Peng Jin(金鹏), Wei-Ying Wang(王维颖), De-Feng Mao(毛德丰), Xu Pan(潘旭), Xiao-Liang Wang(王晓亮), Zhan-Guo Wang(王占国)
Chin. Phys. B . 2017, 26(7): 077802. **doi:** 10.1088/1674-1056/26/7/077802

Review of ultrafast spectroscopy studies of valley carrier dynamics in two-dimensional semiconducting transition metal dichalcogenides

Dong Sun(孙栋), Jia-Wei Lai(赖佳伟), Jun-Chao Ma(马骏超), Qin-Sheng Wang(王钦生), Jing Liu (刘晶)
Chin. Phys. B . 2017, 26(3): 037801. **doi:** 10.1088/1674-1056/26/3/037801

Spin-valley Hall conductivity of doped ferromagnetic silicene under strain

Bahram Shirzadi, Mohsen Yarmohammadi
Chin. Phys. B . 2017, 26(1): 017203. **doi:** 10.1088/1674-1056/26/1/017203

Effect of strain on exciton dynamics in monolayer WS_2*

Lu Zhang(张璐), Da-Wei He(何大伟), Jia-Qi He(何家琪)†, Yang Fu(付洋), and Yong-Sheng Wang(王永生)‡

Key Laboratory of Luminescence and Optical Information, Ministry of Education, Institute of Optoelectronic Technology, Beijing Jiaotong University, Beijing 100044, *China*

(Received 8 April 2019; revised manuscript received 19 May 2019; published online 9 July 2019)

The exciton dynamics in a WS_2 monolayer with strain are studied by transient absorption measurements. We measure the differential transmission signal from monolayer WS_2 as a function of the probe wavelength at different levels of strain applied to the sample. The differential transmission spectrum has a positive maximum value at about 614 nm and shows no significant strain dependence. By time-resolving the differential transmission signal, we find that the strain has a minimal effect on the exciton formation process. However, the exciton lifetime is significantly reduced by strain. These results provide useful information for applications of WS_2 in flexible electronic and optoelectronic devices where strain is inevitable.

Keywords: transient absorption, transition metal dichalcogenides, excitons, strain

PACS: 72.80.Ga, 78.20.–e, 78.47.jb, 78.47.jg **DOI:** 10.1088/1674-1056/28/8/087201

1. Introduction

Since graphene was successfully exfoliated in 2004,[1] it has attracted a lot of attention, owing to its excellent electronic properties that are attractive for many applications.[2,3] Due to the lack of a bandgap of graphene, which is desirable for logic electronics and optoelectronics, the interest in two-dimensional (2D) materials has expanded to other layered materials such as transition metal dichalcogenides (TMDs).[4–6] TMDs are layered materials with a formula of MX_2, where M denotes a transition metal atom (Mo, W) and X refers to a chalcogenide atom (S, Se, Te).[7,8] With their ultrathin bodies and unique thickness-dependent bandgaps, TMDs are expected to be widely used in electrical circuits,[9–11] photodetectors,[12–14] and photovoltaic devices.[15–17]

WS_2 is one of the representative semiconducting TMDs, with a bandgap in the range of 1.3 eV–2.0 eV.[18,19] Bulk WS_2 exhibits an indirect bandgap of 1.3 eV. With the number of layers decreasing, monolayer WS_2 becomes a direct semiconductor with a bandgap of 2.0 eV.[20] Theoretical calculations predicted that WS_2 has high charge mobility among the semiconducting TMDs due to the reduced effective mass.[21] The high photoluminescence (PL) yield of monolayer WS_2 is attractive to applications in optoelectronic devices demanding high quantum efficiency.[22] With these excellent optical and electronic properties, WS_2 is expected to be widely used in electronic and optoelectronic devices.[23–27]

The physical properties of TMDs depend on the band structure. As such, the strain can be used to modulate the band structure and thus tune the physical properties of TMDs.[28,29] Recently, the effect of strain in TMDs has been investigated extensively both theoretically and experimentally.[30–32] Theoretical calculations show that for TMD monolayers with 1T structures, such as HfS_2 and $HfSe_2$, the uniform isotropic strain in a range from -5% to 5% of their bandgap can increase, while for 2H TMDs the bandgap decreases linearly as the lattice constant increases.[33] When applying a uniaxial strain, the results are similar but have a smaller modulation of the bandgap.[34] Recent experiments indicated that the A-exciton exhibits a redshift under a rate of 46 meV/% strain for WS_2.[35] The PL yield for bilayer WSe_2 is improved dramatically under uniaxial strain, making it comparable to unstrained monolayer WSe_2 due to an indirect-to-direct bandgap transition for strained bilayer WSe_2.[36] TMD field-effect transistors (FETs) have been fabricated on flexible substrates and the effect of strain has been studied.[37,38]

Exciton dynamics in monolayer TMDs play an important role in determining their electronic and optical properties, and have been studied using transient absorption measurements.[39–43] However, the effect of strain on excitons dynamics has been less explored. In this paper, we report a transient absorption measurement of exciton dynamics in monolayer WS_2 that is subjected to various levels of strain. These results provide useful information for application as TMDs in flexible electronic and optoelectronic devices are inevitably subjected to strain.

*Project supported by the National Key Research and Development Program of China (Grant No. 2016YFA0202302), the National Natural Science Foundation of China (Grant Nos. 61527817 and 61875236), the Initiative Postdocs Supporting Program of China (Grant No. BX201600013), the General Financial Grant from the China Postdoctoral Science Foundation (Grant No. 2017M610756), the Overseas Expertise Introduction Center for Discipline Innovation, China, and the 111 Center of China.

†Corresponding author. E-mail: jqhe@bjtu.edu.cn

‡Corresponding author. E-mail: yshwang@bjtu.edu.cn

© 2019 Chinese Physical Society and IOP Publishing Ltd

2. Experiment

Monolayer WS_2 samples were obtained by micromechanical exfoliation of bulk material on a thin polydimethylsiloxane (PDMS) flexible substrate. Their monolayer thickness was confirmed by using optical contrast and PL yield. The PL spectrum was measured using a confocal microscope system (LabRAM HR Evolution) with a 50× objective lens, and under the excitation of a 532-nm continuous-wave laser.

The exciton dynamics in monolayer WS_2 samples were studied using a transient absorption technique. The differential transmission setup for the transient absorption measurements is shown in Fig. 1(a). An 80-MHz mode-locked Ti:sapphire laser is used to generate 100-fs pulses with a central wavelength of 820 nm. The output of the Ti:sapphire was divided into two parts by a beamsplitter. The majority of the Ti:sapphire output was used to pump an optical parametric oscillator and thus generate a signal output with a central wavelength in the range of 490 nm–750 nm, which was used as the probe pulse. The other part was focused onto a beta barium borate crystal to generate its second harmonic at 410 nm, which was used as the pump pulse. The pump and probe pulse were focused onto the sample surface through a microscope objective lens with a spot size of 1.66 μm and 2.04 μm in full width at half maximum, respectively. The transmitted probe was collimated by another microscope objective lens and was sent to a silicon photodiode. A set of filters was used to block the pump pulse in front of the photodiode. A lock-in amplifier was used to measure the voltage output of the photodiode. The pump pulse was modulated by a mechanical chopper at 2 kHz. The voltage measured by the lock-in amplifier was proportional to the differential transmission of the probe, $\Delta T/T_0$. This quantity is defined as $\Delta T/T_0 = (T - T_0)/T_0$, where T and T_0 are the transmission coefficient of the sample with the pump presence and without it, respectively. The differential transmission was measured as a function of the probe delay, which is defined as the time delay of the probe pulse with respect to the pump pulse and can be controlled by changing the length of the pump path with a linear motor stage.

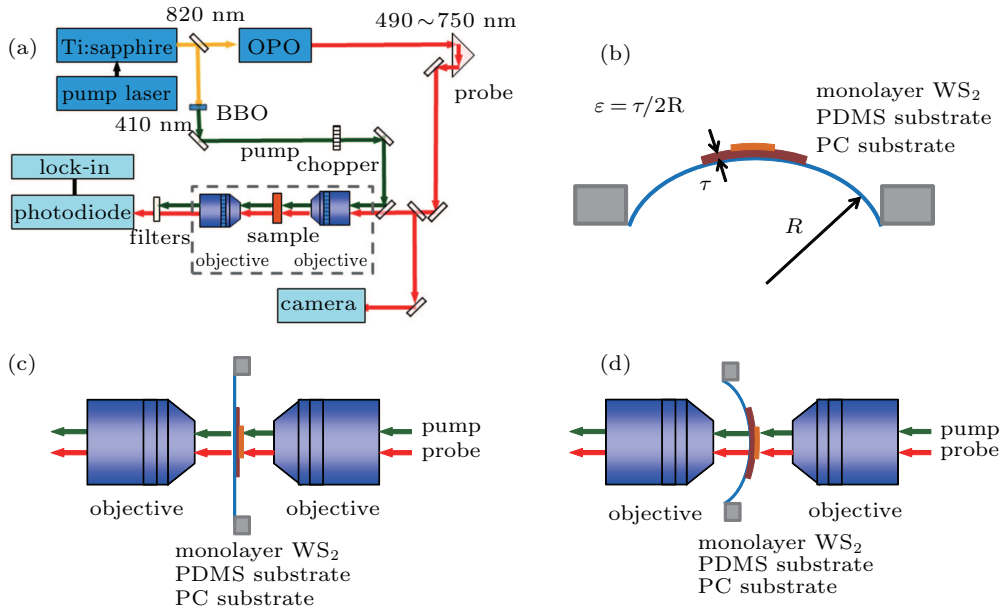


Fig. 1. (a) Schematics of differential transmission setup for transient absorption measurements. (b) Schematic drawing of two-point bending apparatus along with the method to calculate strain. Setup of bending apparatus (c) without and (d) with strain corresponding to gray dashed box in panel (a).

A two-point bending apparatus[36,44] was used to apply uniaxial tensile strain to the monolayer WS_2 flakes as shown in Fig. 1(b). The monolayer WS_2 flakes and small PDMS film were located at the central part of a polycarbonate (PC) flexible substrate. The PC substrate was located between two screw posts. The PDMS substrate was attached to the PC substrate and therefore had uniaxial tensile strain on its top surface. It can be shown that the applied strain was $\varepsilon = \tau/2R$,[35,45] where τ is the thickness of the PDMS substrate and R the radius of the PDMS substrate as shown in Fig. 1(b).

The setup of the bending apparatus without strain and with different levels of strain in the transient absorption system are shown in Figs. 1(c) and 1(d), respectively. Uniaxial tensile strain was obtained by changing the distance between the two translation stages. When the substrate was bent, the entire sample mount was moved so that the sample remained at the focal plane of both objective lenses. By using this setup, we could measure the differential transmission with various values of strain. All the measurements were performed under ambient conditions.

3. Results and discussion

Figure 2(a) shows an optical microscope image of a WS_2 flake. The monolayer region, indicated in the figure, is identified by its green channel contrast of 8.3%, according to previously established values for TMD monolayers on thick and transparent substrates.[46] Furthermore, figure 2(c) shows a PL spectrum measured from the monolayer region. Its yield and spectral shape are both consistent with previously reported spectra of monolayer WS_2.[18,47–49] When the laser spot is located in other thin regions of the flake, no PL is detected under the same conditions.

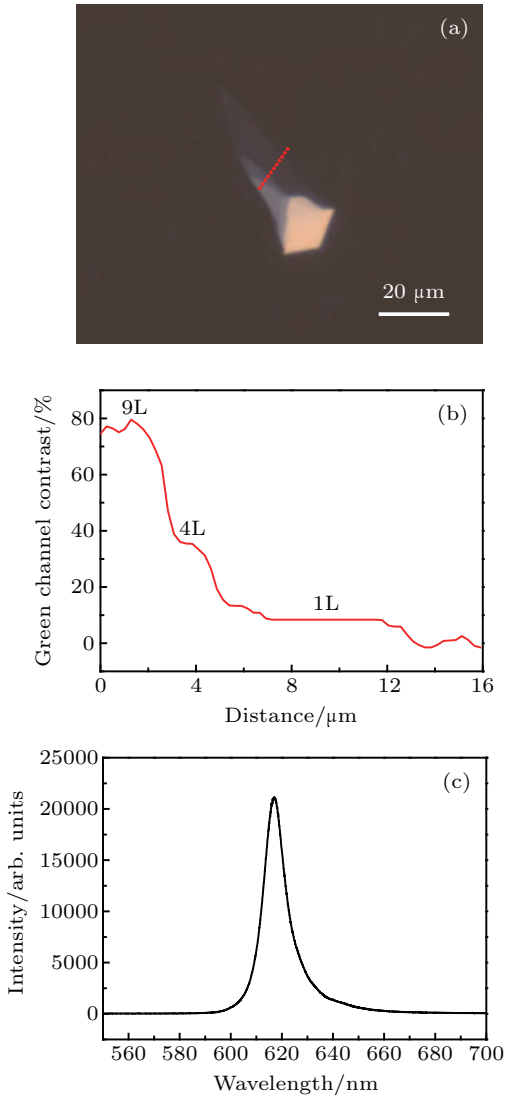


Fig. 2. (a) Optical microscope image of the WS_2 sample. (b) Optical contrast of green channel along red dashed line in panel (a). (c) PL spectrum of monolayer WS_2 sample without strain.

We study the exciton dynamics in monolayer WS_2 with different probe wavelengths and different levels of strain. Firstly, the monolayer WS_2 sample and the PDMS film (with a size of 2 cm×2 cm and a thickness of 0.092 cm) are mounted on the central part of the PC substrate (with a length of 12 cm) as shown in Fig. 1(c) without strain. A 410-nm pump pulse with a peak fluence of 9.9 μJ·cm^{-2} injects photocarriers into the monolayer WS_2 via interband absorption. The dynamics of the injected carriers are monitored by a probe pulse with a photon energy near the PL peak. To apply uniaxial tensile strain to the monolayer WS_2 flake, we change the distance between the two translation stages shown in Fig. 1(d). The distance is changed from 12 cm (without strain) to 11.6 cm, 11.2 cm, and 10.8 cm. According to the length of the PC substrate and the distance between the two translation stages, we can calculate R based on geometrical relations. For example, when the distance is 11.6 cm, R is 13.35 cm. According to the formula $\varepsilon = \tau/2R$, the applied strain is 0.345%. When the distances are 11.2 cm and 10.8 cm, strains are 0.489% and 0.603%, respectively.

Figure 3 shows the peak differential transmission, obtained with probe delay being near zero, from the monolayer WS_2 as a function of the probe wavelength at different levels of strain (symbols, left axis). For comparison, the PL spectrum is also plotted there. Both positive (photobleaching) and negative (photoinduced absorption) signals are observed around the A-exciton resonance, which is consistent with previous studies.[49,50] At all the levels of strain studied, the peak differential transmission has a positive maximum value at about 614 nm, showing no significant strain dependence. This is, however, reasonable, since the expected change of the optical bandgap is on the order of 10 meV with strains of these levels.[35]

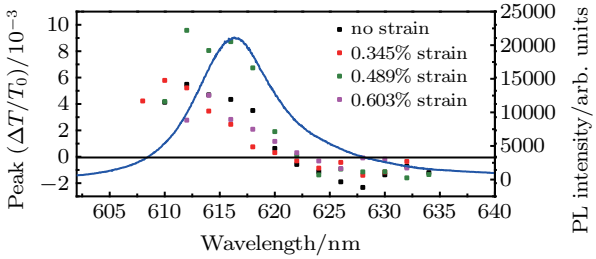


Fig. 3. Peak differential transmission from the monolayer WS_2 as a function of probe wavelength without strain and with different strain (symbols, left axis) and PL of the same sample without strain under 532-nm laser excitation.

Next, we use a 410-nm pump pulse with a peak fluence of 4.95 μJ·cm^{-2} to inject photocarriers and a 614-nm probe to study temporal dynamics of the photocarriers. The results are summarized in Figs. 4(a) and 4(b) for long and short time ranges, respectively. The decay of the signal can be fitted by bi-exponential functions, $\Delta T/T_0 = A_1 \exp(-t/\tau_1) + A_2 \exp(-t/\tau_2) + B$ as indicated by the red lines in Fig. 4(a). The decay time constants obtained from the fits as a function of strain are shown in Fig. 5. The ratio of the amplitudes, A_1/A_2, is from about 2.1 to 3.4 for all levels of strain. The short time constant τ_1 is about 0.8 ± 0.1 ps and is nearly independent of strain. The long time constant τ_2 changes from about 90 ps without strain to about 45 ps with 1.545% strain.

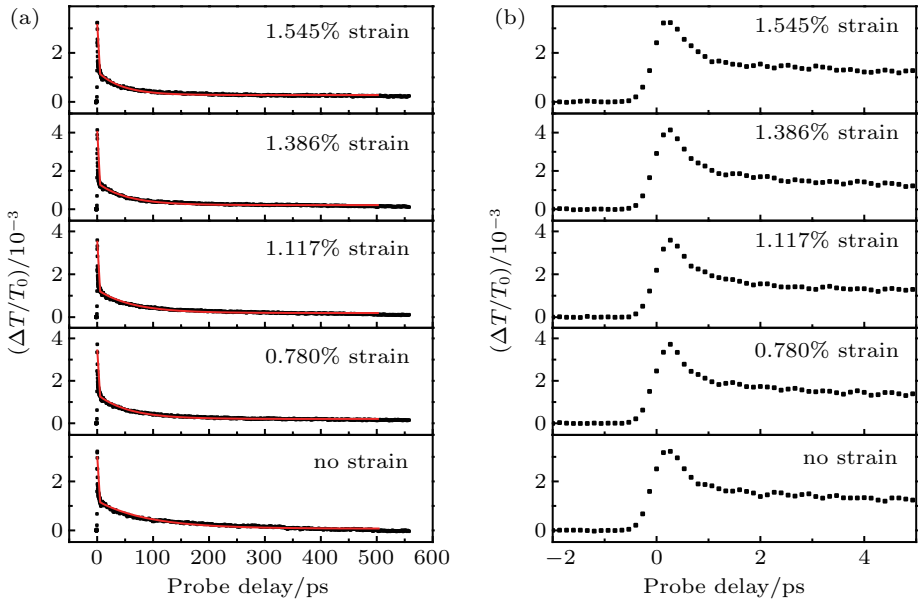


Fig. 4. (a) Differential transmission signals of monolayer WS_2 measured with a 410-nm pump and 614-nm probe pulses without strain and with different strains. The red lines are fitted by bi-exponential functions. (b) The same signal but in a smaller range of the probe delay.

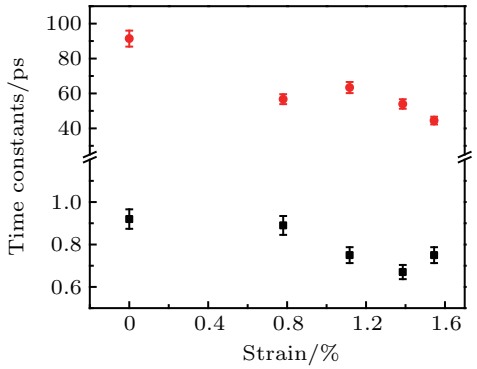


Fig. 5. Decay time constants as a function of strain, obtained from the fits shown in Fig. 4(a).

Previous studies have established that the short and long decay time are associated with the exciton formation and recombination process in TMD monolayers, respectively.[51,52] The 410-nm pump pulse injects free electron–hole pairs. Due to the enhanced Coulomb interaction with reduced dielectric screening in monolayer WS_2, the electrons and holes form excitons rapidly. Since the free electron–hole pairs produce a stronger transient absorption than excitons of the same density, the signal decreases initially as reflected by τ_1. Our results suggest that the strain has a minimal effect on the exciton formation process. The long decay constant determines the exciton recombination lifetime. Hence, our results show that even with a relatively small strain, the lifetime is reduced by about half. The physics mechanism of the exciton lifetime reduction by strain can be attributed to the funneling of excitons to sample locations with higher strain, where they become localized with an enhanced recombination rate. Since exciton lifetime is a key parameter determining the performance of optoelectronic devices, such as the power conversion efficiency of photovoltaic devices, detectivity and response time of photodiodes, and efficiency of LEDs, our results provide important information for the application of TMDs in flexible devices and other devices with strain.

4. Conclusions

In summary, we have performed transient absorption measurements of exciton dynamics in TMDs with strain. We measured differential transmission signals from monolayer WS_2 as a function of the probe wavelength in cases with strain at different levels and without strain, respectively. At all the levels of strain studied, the peak differential transmission had a positive maximum value at about 614 nm, showing no significant strain dependence. By time-resolving the differential transmission signal, we found that the results suggest that the strain has a minimal effect on the exciton formation process; however, even a strain of about 1.5% reduces the exciton lifetime by a factor of about two. These results provide useful information for applications of TMDs in flexible electronic and optoelectronic devices.

References

[1] Novoselov K S, Geim A K, Morozov S V, Jiang D, Zhang Y, Dubonos S V, Grigorieva I V and Firsov A A 2004 *Science* **306** 666
[2] Geim A K and Novoselov K S 2007 *Nat. Mater.* **6** 183
[3] Tian H, Tan Z, Wu C, Wang X, Mohammad M A, Xie D, Yang Y, Wang J, Li L J, Xu J and Ren T L 2014 *Sci. Rep.* **4** 5951
[4] Wang Q H, Kalantar-Zadeh K, Kis A, Coleman J N and Strano M S 2012 *Nat. Nanotechnol.* **7** 699
[5] Jariwala D, Sangwan V K, Lauhon L J, Marks T J and Hersam M C 2014 *ACS Nano* **8** 1102
[6] Kozawa D, Kumar R, Carvalho A, Kumar Amara K, Zhao W, Wang S, Toh M, Ribeiro R M, Castro Neto A H, Matsuda K and Eda G 2014 *Nat. Commun.* **5** 4543

[7] Wilson J A and Yoffe A D 1969 *Adv. Phys.* **18** 193
[8] Ataca C, Sahin H and Ciraci S 2012 *J. Phys. Chem. C* **116** 8983
[9] Radisavljevic B, Whitwick M B and Kis A 2011 *ACS Nano* **5** 9934
[10] Baugher B W H, Churchill H O H, Yang Y and Jarillo-Herrero P 2014 *Nat. Nano* **9** 262
[11] Cheng R, Jiang S, Chen Y, Liu Y, Weiss N, Cheng H C, Wu H, Huang Y and Duan X 2014 *Nat. Commun.* **5** 5143
[12] Yin Z, Li H, Li H, Jiang L, Shi Y, Sun Y, Lu G, Zhang Q, Chen X and Zhang H 2012 *ACS Nano* **6** 74
[13] Lopez-Sanchez O, Lembke D, Kayci M, Radenovic A and Kis A 2013 *Nat. Nanotechnol.* **8** 497
[14] Cui S M, Pu H H, Wells S A, Wen Z H, Mao S, Chang J B, Hersam M C and Chen J H 2015 *Nat. Commun.* **6** 8632
[15] Tsai M L, Su S H, Chang J K, Tsai D S, Chen C H, Wu C I, Li L J, Chen L J and He J H 2014 *ACS Nano* **8** 8317
[16] Yun J M, Noh Y J, Lee C H, Na S I, Lee S, Jo S M, Joh H I and Kim D Y 2014 *Small* **10** 2319
[17] Gourmelon E, Lignier O, Hadouda H, Couturier G, Bernede J C, Tedd J, Pouzet J and Salardenne J 1997 *Sol. Energy Mater. Sol. Cells* **46** 115
[18] Gutierrez H R, Perea-Lopez N, Elias A L, Berkdemir A, Wang B, Lv R, Lopez-Urias F, Crespi V H, Terrones H and Terrones M 2013 *Nano Lett.* **13** 3447
[19] Braga D, Lezama I G, Berger H and Morpurgo A F 2012 *Nano Lett.* **12** 5218
[20] Elias A L, Perea-Lopez N, Castro-Beltran A, Berkdemir A, Lv R T, Feng S M, Long A D, Hayashi T, Kim Y A, Endo M, Gutierrez H R, Pradhan N R, Balicas L, Houk T E M, Lopez-Urias F, Terrones H and Terrones M 2013 *ACS Nano* **7** 5235
[21] Liu L, Kumar S B, Ouyang Y and Guo J 2011 *IEEE Trans. Electron. Dev.* **58** 3042
[22] Weijie Z, Zohreh G, Leiqiang C, Minglin T, Christian K, Ping-Heng T and Goki E 2013 *ACS Nano* **7** 791
[23] Sang Y H, Zhao Z H, Zhao M W, Hao P, Leng Y H and Liu H 2015 *Adv. Mater.* **27** 363
[24] Perea-Lopez N, Elias A L, Berkdemir A, Castro-Beltran A, Gutierrez H R, Feng S M, Lv R T, Hayashi T, Lopez-Urias F, Ghosh S, Muchharla B, Talapatra S, Terrones H and Terrones M 2013 *Adv. Funct. Mater.* **23** 5511
[25] Shanmugam M, Bansal T, Durcan C A and Yu B 2012 *Appl. Phys. Lett.* **101** 263902
[26] Cui Y, Xin R, Yu Z H, Pan Y M, Ong Z Y, Wei X X, Wang J Z, Nan H Y, Ni Z H, Wu Y, Chen T S, Shi Y, Wang B G, Zhang G, Zhang Y W and Wang X R 2015 *Adv. Mater.* **27** 5230
[27] Lan C Y, Li C, Yin Y and Liu Y 2015 *Nanoscale* **7** 5974
[28] Wang Y L, Cong C X, Yang W H, Shang J Z, Peimyoo N, Chen Y, Kang J Y, Wang J P, Huang W and Yu T 2015 *Nano Res.* **8** 2562
[29] Zhang Q, Chang Z, Xu G, Wang Z, Zhang Y, Xu Z Q, Chen S, Bao Q, Liu J Z and Mai Y W 2016 *Adv. Funct. Mater.* **26** 8707
[30] Kou L, Du A, Chen C and Frauenheim T 2014 *Nanoscale* **6** 5156
[31] Yu S, Zhu H, Eshun K, Shi C, Zeng M and Li Q 2016 *Appl. Phys. Lett.* **108** 191901
[32] Li M, Dai J and Zeng X C 2015 *Nanoscale* **7** 15385
[33] Guzman D M and Strachan A 2014 *J. Appl. Phys.* **115** 243701
[34] Maniadaki A E, Kopidakis G and Remediakis I N 2016 *Solid State Commun.* **227** 33
[35] He X, Li H, Zhu Z, Dai Z, Yang Y, Yang P, Zhang Q, Li P, Schwingenschlogl U and Zhang X 2016 *Appl. Phys. Lett.* **109** 173105
[36] Desai S B, Seol G, Kang J S, Fang H, Battaglia C, Kapadia R, Ager J W, Guo J and Javey A 2014 *Nano Lett.* **14** 4592
[37] Lee G H, Yu Y J, Cui X, Petrone N, Lee C H, Choi M S, Lee D Y, Lee C, Yoo W J and Watanabe K 2013 *ACS Nano* **7** 7931
[38] Shen T, Penumatcha A V and Appenzeller J 2016 *ACS Nano* **10** 4712
[39] He J Q, He D W, Wang Y S, Cui Q N, Ceballos F and Zhao H 2015 *Nanoscale* **7** 9526
[40] Cui Q, He J, Bellus M Z, Mirzokarimov M, Hofmann T, Chiu H Y, Antonik M, He D, Wang Y and Zhao H 2015 *Small* **11** 5565
[41] Cui Q N, Ceballos F, Kumar N and Zhao H 2014 *ACS Nano* **8** 2970
[42] Kumar N, Cui Q N, Ceballos F, He D W, Wang Y S and Zhao H 2014 *Phys. Rev. B* **89** 125427
[43] Kumar N, Cui Q, Ceballos F, He D, Wang Y and Zhao H 2014 *Nanoscale* **6** 4915
[44] Isl, J O, Kuc A, Diependaal E H, Bratschitsch R, van der Zant H S, Heine T and Castellanos-Gomez A 2016 *Nanoscale* **8** 2589
[45] Schmidt R, Niehues I, Schneider R, Drüppel M, Deilmann T, Rohlfing M, de Vasconcellos S M, Castellanos-Gomez A and Bratschitsch R 2016 *2D Materials* **3** 021011
[46] Cui Q, Muniz R A, Sipe J E and Zhao H 2017 *Phys. Rev. B* **95** 165406
[47] Zhao W J, Ribeiro R M, Toh M L, Carvalho A, Kloc C, Neto A H C and Eda G 2013 *Nano Lett.* **13** 5627
[48] Peimyoo N, Shang J Z, Cong C X, Shen X N, Wu X Y, Yeow E K L and Yu T 2013 *ACS Nano* **7** 10985
[49] He J, Kumar N, Bellus M Z, Chiu H Y, He D, Wang Y and Zhao H 2014 *Nat. Commun.* **5** 5622
[50] Pan S, Ceballos F, Bellus M Z, Zereshki P and Zhao H 2016 *2D Materials* **4** 015033
[51] Ceballos F, Cui Q, Bellus M Z and Zhao H 2016 *Nanoscale* **8** 11681
[52] Ceballos F and Zhao H 2017 *Adv. Funct. Mater.* **27** 1604509